

AI for Next-Generation Wireless Networks: Communication and Computation Resource Management, and Channel Estimation

Dr. Yuanjian Li

Research Fellow at Nanyang Technological University (NTU), Singapore
PhD in Telecommunications from King's College London (KCL), the UK

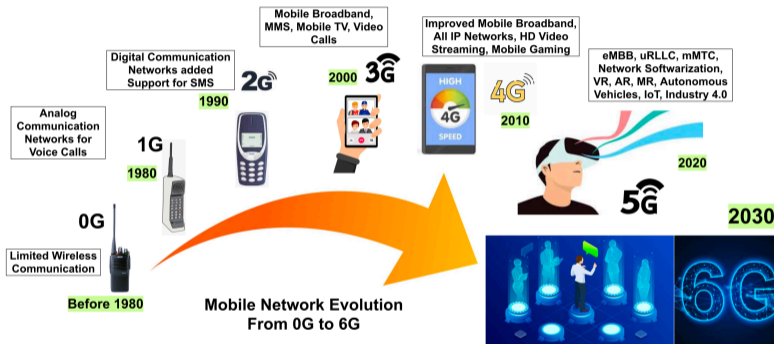
September 6, 2024



Table of Contents

- ➊ Introduction to the Next-Generation Wireless Networks (∼8 min)
- ➋ Quantum-Aided DRL for Cellular-Connected UAV Path Planning (∼10 min)
- ➌ Multi-Agent DRL for UAV-Aided Task Offloading in IoT (∼10 min)
- ➍ Channel Estimation for THz UM-MIMO (∼15 min)
- ➎ Quantum Machine Learning for Next-Gen Wireless Systems (∼7 min)
- ➏ Q&A (∼10 min)

The History of Wireless Communications



6G Requirements:

Peak Data rate > 1 Tbps, End-to-end delay < 0.1 ms, Processing delay < 10 ns, Reliability > 99.99999%, Availability > 99.99999%, Connection Density > 10^7 Devices/km², Energy Efficiency > 100x over 5G, Spectrum Efficiency > 5x over 5G, Mobility > 1000 kmph

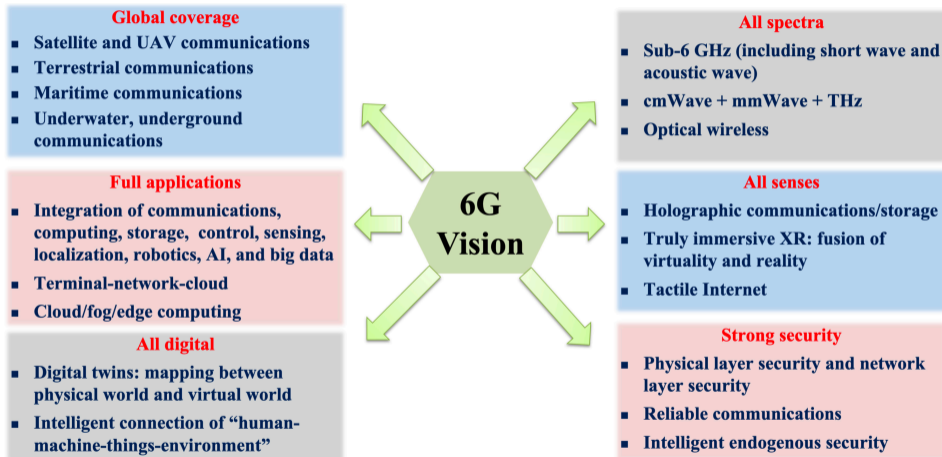
6G Vision: FeMBB, umMTC, eRLLC/eURLLC, ELPC, LDHMC, High Spectrum Efficiency, High Area Traffic Capacity, MBBLL, mLMT, AEC

6G Enablers: THz Spectrum, AI and Federated Learning, Compressive Sensing, Blockchain/DLT, Swarm Networking, Zero Touch Network and Service Management, Efficient Energy Transfer and Harvesting, Smart Surfaces, NTN Towards 3D Networking, VLC, Quantum Communication

6G Applications: UAV, Holographic Telepresence, Extended Reality, Collaborative Autonomous Driving, Internet of Everything, Smart Grid 2.0, Industry 5.0, Hyper-intelligent IoT, Collaborative Robots, Personalized Body Area Networks, Intelligent Healthcare, Space and Deep-Sea Tourism

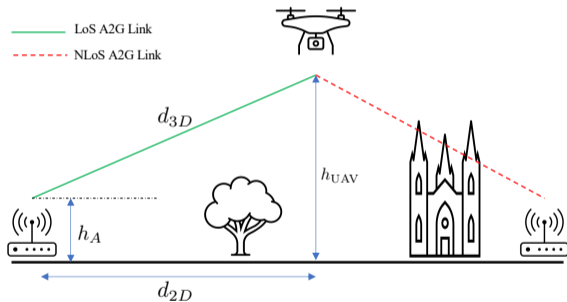
C. De Alwis, A. Kalla, Q.-V. Pham, P. Kumar, K. Dev, W.-J. Hwang, and M. Liyanage, "Survey on 6G frontiers: Trends, applications, requirements, technologies and future research," *IEEE Open J. Commun. Soc.*, vol. 2, pp. 836–886, 2021.

The Next-Gen (6G) Wireless Systems



C.-X. Wang, X. You, X. Gao, X. Zhu, Z. Li, C. Zhang, H. Wang, Y. Huang, Y. Chen, H. Haas et al., “On the road to 6G: Visions, requirements, key technologies, and testbeds,” *IEEE Communications Surveys & Tutorials*, vol. 25, no. 2, pp. 905–974, 2023.

Why UAV-Aided Network?



- Enhanced coverage and connectivity
- More likely to establish line-of-sight (LoS) air-to-ground (A2G) wireless links due to high altitude
- Configurable mobility and on-demand deployment
- Support for IoT & smart applications

Some Examples of UAV-Assisted IoT Application Scenarios

Smart City

- Surveillance
- Delivery
- Intelligent transportation system



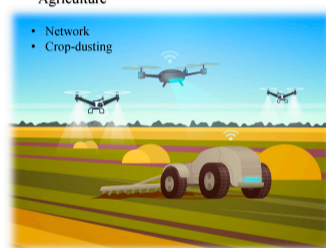
Disaster and Emergency

- Network
- Delivery
- Surveillance



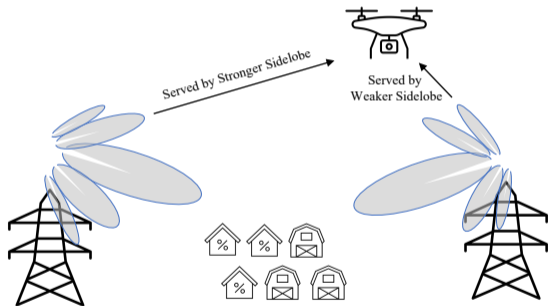
Agriculture

- Network
- Crop-dusting



SN. Cheng, S. Wu, X. Wang, Z. Yin, C. Li, W. Chen, and F. Chen, "AI for UAV-assisted IoT applications: A comprehensive review," *IEEE Internet Things J.*, vol. 10, no. 16, pp. 14 438–14 461, 2023.

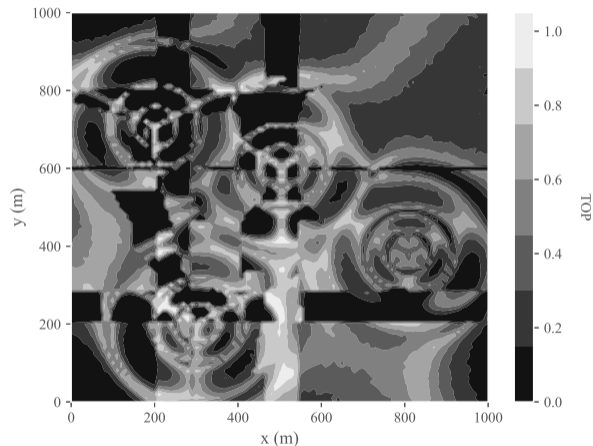
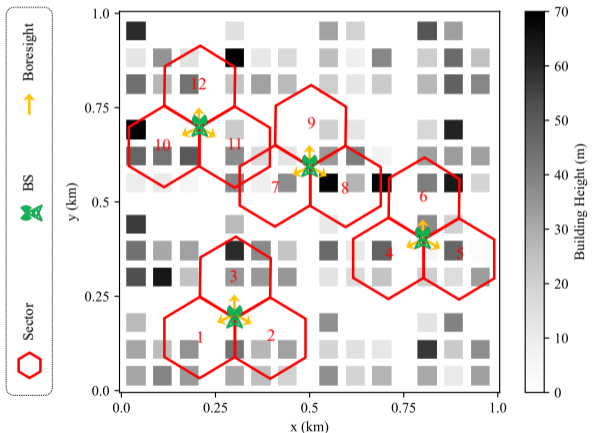
What is Cellular-Connected UAVs Networks?



- Beyond visual and radio LoS (BVR-LoS) communications
- Reuse cellular networks thus cost-effective
- Compensate GPS coverage for better UAV navigation
- Main lobes of terrestrial base stations (BSs) are downtitled towards ground
- UAVs can be served by side lobes

The Cellular-Connected UAV Environment

Example: Parcel Collection to the Distribution Centre of Delivery Firm

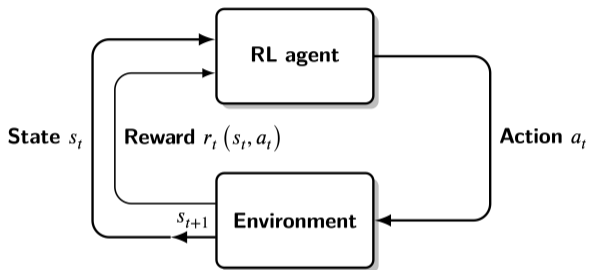


What is Reinforcement Learning and How It Works?

ChatGPT

Tesla Autopilot

AlphaGO



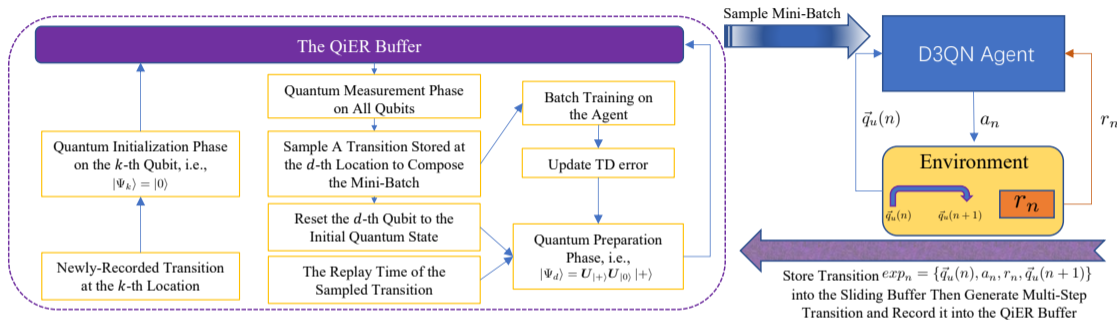
Reinforcement learning works by allowing an agent to learn optimal behavior through trial and error, receiving feedback in the form of rewards from its environment to achieve intelligent decision making.

$$Q_u(s, a|\pi) = \mathbb{E}\left[\sum_{t=0}^{+\infty} \gamma^t r_{u,t+1} | s_0 = s, a_0 = a, \pi\right]$$

To find the optimal policy π that can maximize the long-term accumulated discounted rewards Q_u .

- **State (s_t):** Agent's current state
- **Action (a_t):** Agent's selected action
- **Reward (r_t):** The feedback from the environment based on the action taken
- **Next State (s_{t+1}):** The next state the agent would be in

The Proposed Quantum-Enhanced Deep Reinforcement Learning Algorithm

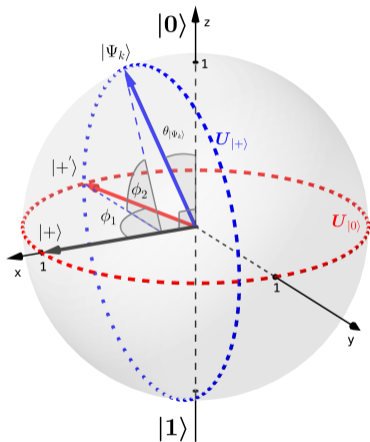


3 phases: **Quantum Initialization**, **Quantum Preparation**, and **Quantum Measurement**

Associate the quantum collapse distribution with the probability whether picking one particular experience sample from the buffer

QiER is short for quantum-inspired experience replay, which invokes quantum computing to aid in DRL learning frameworks.

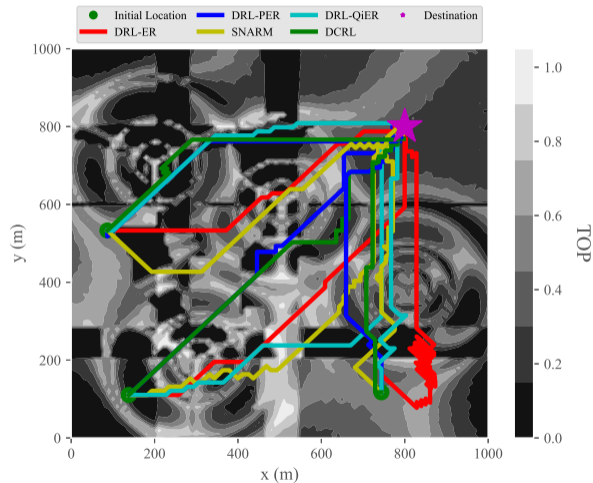
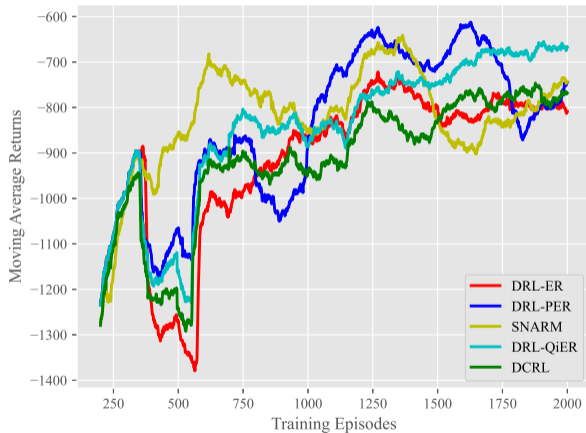
How Quantum-Inspired Experience Replay Works?



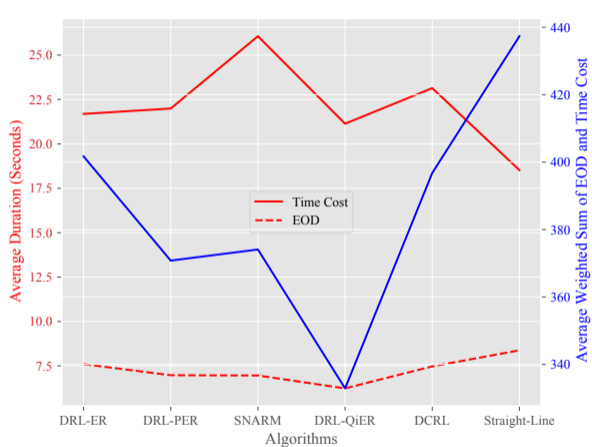
$$|\Psi_c\rangle = |\Psi_1\rangle \otimes |\Psi_2\rangle \otimes \cdots \otimes |\Psi_{\hat{n}}\rangle = \sum_{p=00\dots 0}^{\overbrace{11\dots 1}^{\hat{n}}} h_p |p\rangle$$

- Quantum superposition: $|\Psi\rangle = \alpha |0\rangle + \beta |1\rangle$
- Probability amplitude: $\alpha = \langle 0|\Psi\rangle$, $\beta = \langle 1|\Psi\rangle$
- $|\alpha|^2 + |\beta|^2 = 1$
- After measurement, $|\Psi\rangle$ will collapse onto one of its eigenstates $|0\rangle$ and $|1\rangle$ with probabilities $|\alpha|^2$ and $|\beta|^2$, respectively.
- The idea is to use Grover iteration from quantum computing to manipulate the collapse distribution

Training Return History and Designed UAV Trajectories



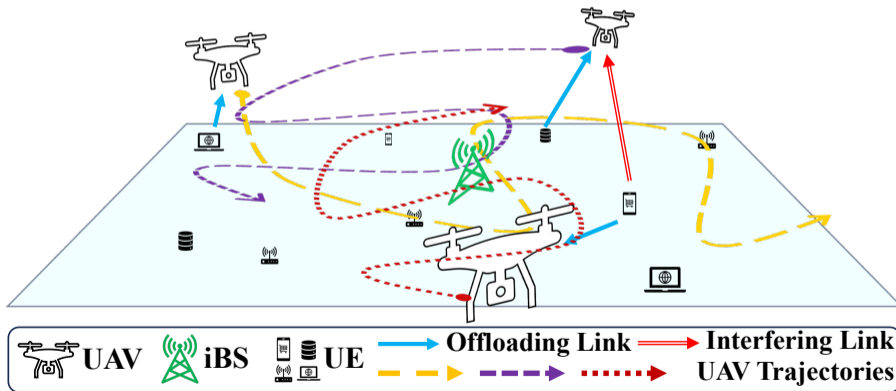
Performance Comparison on Ergodic Outage Duration (EOD) and Time Cost



	Circular	BS-Approaching	DRL-QiER
Time Cost	28.440 s	31.916 s	31.234 s
EOD	10.469 s	12.128 s	8.136 s
Weighted Sum of Time Cost and EOD	551.890	638.316	438.034

System Model Diagram of Many-UAV-Enabled Computation Offloading for Terrestrial IoT Users

Multiple unmanned aerial vehicles (UAVs) are deployed to provide energy-limited computation-scarce terrestrial IoT user equipments (UEs) with accessible task offloading services.



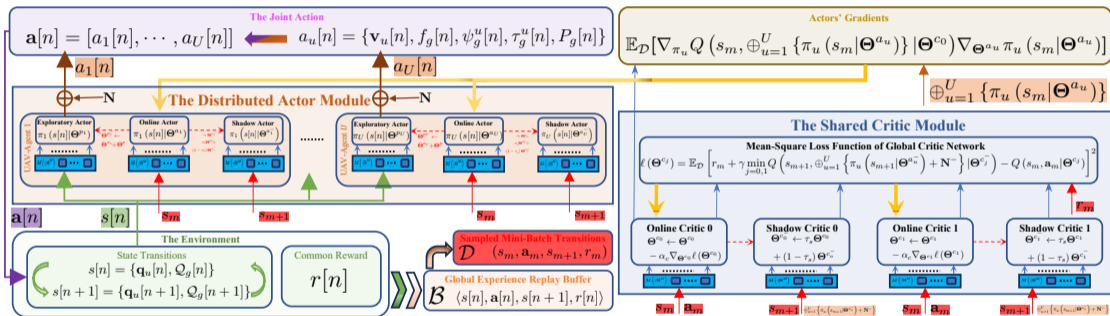
Mang-Agent Deep Reinforcement Learning (MADRL)-Aided Communication and Computing Resource Coordination for Multi-Access Edge Computing (MEC) Systems

This work focuses on developing MADRL-driven strategies to optimize key performance metrics, such as energy efficiency, in MEC systems.

$$\max_{\{\mathbf{v}_u[n], f_g[n], \psi_g^u[n], \tau_g^u[n], P_g[n]\}} \frac{1}{N} \sum_{n=1}^N \frac{d[n]}{E[n]}$$

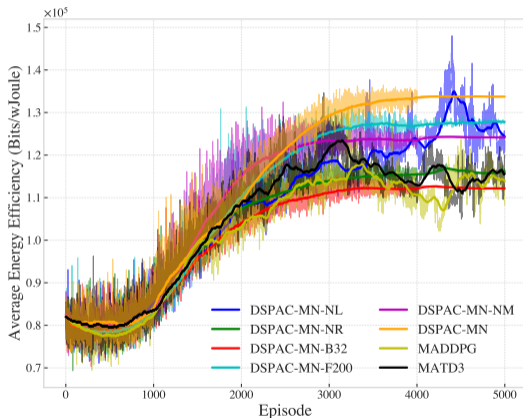
The optimization process jointly considers communication and computation resources, including UAVs' trajectories, UEs' local central processing unit (CPU) clock speeds, UAV-UE associations, time slot slicing, and UEs' offloading powers, after mapping the original problem into a stochastic (Markov) game.

Workflow of the Proposed Duo-Staggered Perturbed Actor-Critic with Modular Networks (DSPAC-MN) Algorithm in MADRL Setups



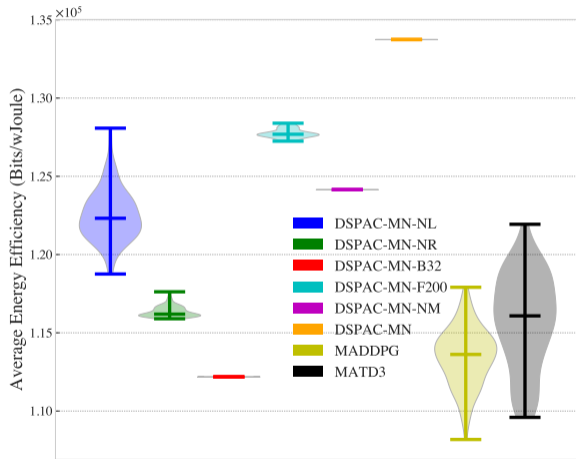
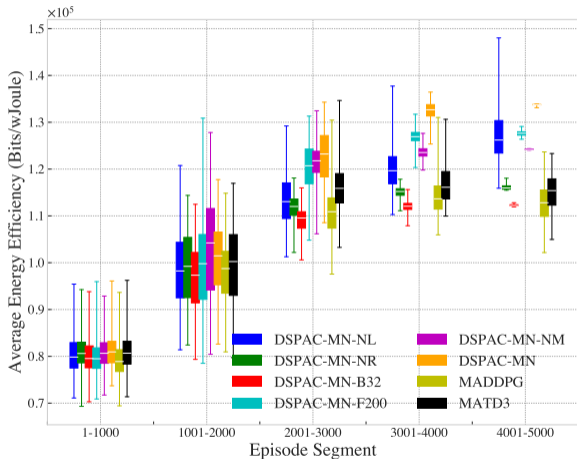
- **Distributed Agents:** explore in parallel
- **Shared Critic:** cooperative learning
- **Modularized Inputs:** balanced dimension
- **Perturbed Actors:** enhanced exploration

Return History of the Online Training Process

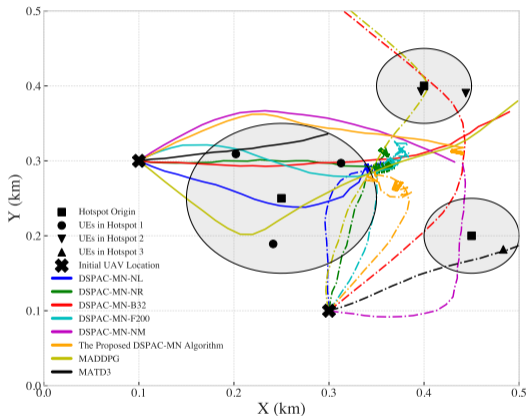


- *MADDPG*: an extension of deep deterministic policy gradient (DDPG) to handle multi-agent scenarios
- *MATD3*: an extension of twin-delayed DDPG (TD3) to reduce overestimation bias of MADDPG
- *DSPAC-MN-NM*: DSPAC-MN without modular networks
- *DSPAC-MN-NR*: Regularization-less DSPAC-MN
- *DSPAC-MN-NL*: DSPAC-MN without learning rate scheduling
- *DSPAC-MN-B32*: DSPAC-MN with batch size of 32
- *DSPAC-MN-F200*: DSPAC-MN with policy renewal frequency of 200

Box and Violin Plots of Performance Comparison on Expected Energy Efficiency

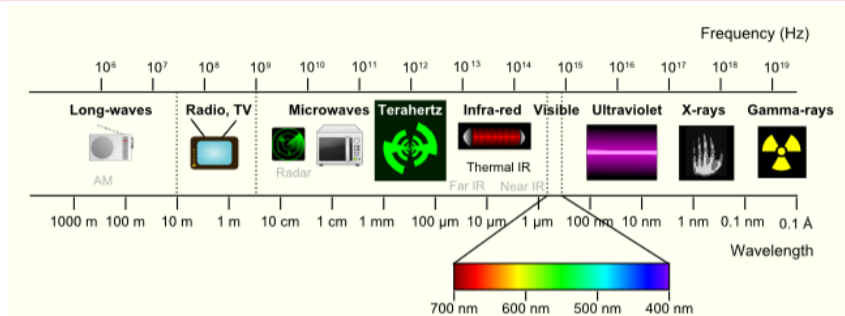


Visualization of and Comparison on Devised Trajectories over Various Algorithms



- the proposed DSPAC-MN solution can generate trajectories that are not only sufficiently separated from each other but also away from the borders
- baselines DSPAC-MN-B32, MADDPG and MATD3 cannot avoid UAVs from **crushing** onto borders
- benchmarks DSPAC-MN-NL, DSPAC-MN-NR, DSPAC-MN-F200 and DSPAC-MN-NM design trajectories that end up **colliding** with each other

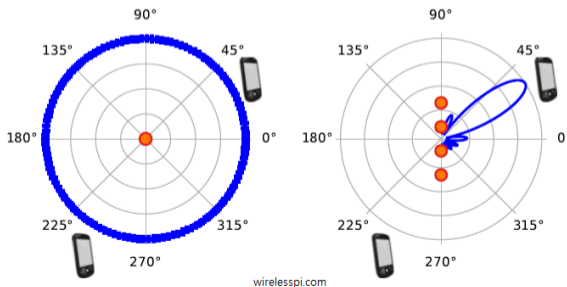
Why Terahertz (THz) Communications?



Terahertz (THz) transmissions, operating in the **0.1-10 THz** frequency range, offer the potential for ultra-high data rates, reaching up to several Terabits per second (**Tbps**) with ultra-broad spectrum blocks (bandwidth). This capability is considered a key building block of the forthcoming 6G communications in supporting applications such as *immersive virtual reality (VR)* and *holographic communications*.

Why Ultra-Massive Multiple-Input Multiple-Output (UM-MIMO) for THz Transmissions?

However, the appealing multi-Gigahertz bandwidth comes with **severe propagation attenuation** due to substantial atmospheric and spreading losses from molecular absorption and high carrier frequency, respectively. An emerging solution to broadening THz transmission coverage is ultra-massive multiple-input multi-output (UM-MIMO) technology, which offers high-level array gain to compensate THz propagation losses by forming pencil-thin directional radiation beams.



An Example of the Large-Scale Path Loss Model on the THz Band

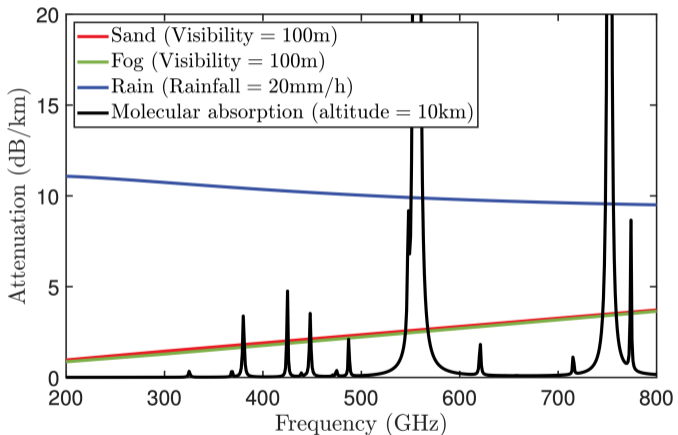
$$\text{PL} [d, f] = \left| \left(\frac{c}{4\pi df} \right) \exp \left[-\frac{1}{2} \kappa (f, \mu) d \right] \exp \left[-j2\pi f \frac{d}{c} \right] \right|^2$$

The equation is annotated with the following labels and arrows:

- Distance** (blue arrow) points to d in the first bracketed term $[d, f]$.
- Carrier Frequency** (red arrow) points to f in the second bracketed term $[d, f]$.
- Speed of Light** (green arrow) points to c in the fraction $\frac{c}{4\pi df}$.
- Molecular Absorption Coefficient** (pink arrow) points to κ .
- the volume of the mixing ratio of water vapor** (olive arrow) points to μ .
- time-of-arrival** (orange arrow) points to $\frac{d}{c}$ in the second exponential term.

Distance-Dependent and Frequency-Selective!

Attenuation versus Frequency for the Different Weather Conditions



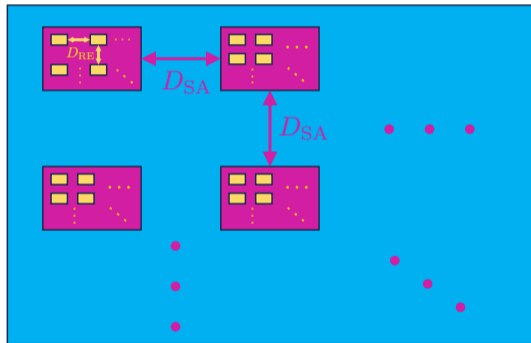
Han, Chong, et al. "Molecular absorption effect: A double-edged sword of terahertz communications." IEEE Wireless Communications (2022).

Machine Learning (ML)-Enabled Channel Estimation for Terahertz (THz) Ultra-Massive Multi-Input-Multi-Output (UM-MIMO) Communications

To facilitate efficient THz communications, UM-MIMO systems that provide substantial beamforming gains are essential. However, tailored channel estimation solutions are necessary to fully leverage UM-MIMO for THz transmissions. This involves practical modeling of the near-field propagation characteristics, molecular absorption, and scatter reflection effects. To address challenges such as angular-domain energy spread and the beam split effect, a **dictionary learning framework** that creates an adaptive sparsifying matrix from the THz channel dataset is proposed. Then, a **Bayesian learning channel estimation** solution is adopted. Furthermore, a **model-driven deep learning** approach is introduced, which unrolls iterative algorithms into a finite-length, layer-wise deep neural network designed to learn the sparse representation of the THz channel from the THz channel dataset and received pilot signals.

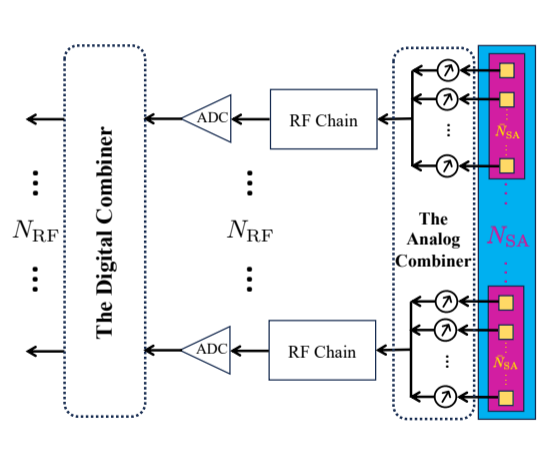
Array-of-Subarray (AoSA)-Based UM-MIMO Architecture

RE
 SA
 AoSA



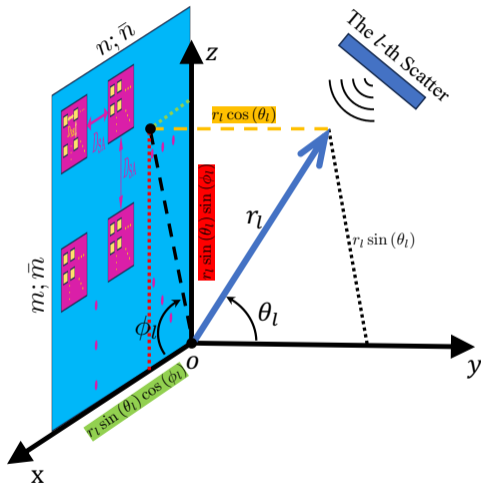
- Each subarray (SA) comprises $\bar{N}_{SA} = \bar{N} \times \bar{M}$ radiating elements (REs), antennas
- The amount of SAs is denoted by $N_{SA} = N \times M$
- The AoSA consists of $A = \bar{N}_{SA} N_{SA}$ antennas/REs in total
- RE displacement $D_{RE} = \lambda_c/2$ in each SA
- SA displacement $D_{SA} = wD_{RE}$, where $w \gg 1$

Partially-Connected Hybrid Combining Scheme



- An energy-efficient hybrid combining strategy are implemented at the AoSA, where REs in each SA share the same RF chain via dedicated analog combiner, in a partially-connected manner, i.e., the amount of RF chains $N_{RF} = N_{SA} \ll A$.
- Following each RF chain, an analog-to-digital converter (ADC) is adopted to sample and quantize the analog waveform, transforming it into digitalized data for baseband signal processing.
- The fully-connected hybrid combining architecture: $N_{RF} \times A$ RF links, while the partially-connected strategy: A links.

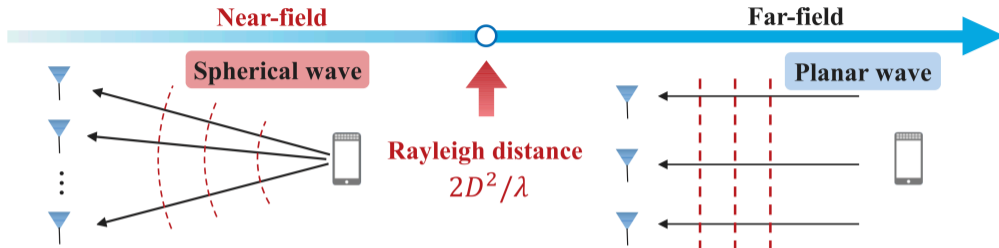
AoSA-Based UM-MIMO with Partially-Connected Hybrid Combining



- $\phi_l \in [-\pi, \pi]$ is the azimuth angle-of-arrival (AoA) and $\theta_l \in [-0.5\pi, 0.5\pi]$ is the elevation AoA of the propagation path from the l -th scatterer to the AoSA's origin
- The location of the l -th scatterer is

$$\mathbf{l}_l = r_l [\sin(\theta_l) \cos(\phi_l), \cos(\theta_l), \sin(\theta_l) \sin(\phi_l)],$$
 where r_l , ϕ_l and θ_l are measured w.r.t. the AoSA origin, i.e., the (1, 1)-th SA's origin.

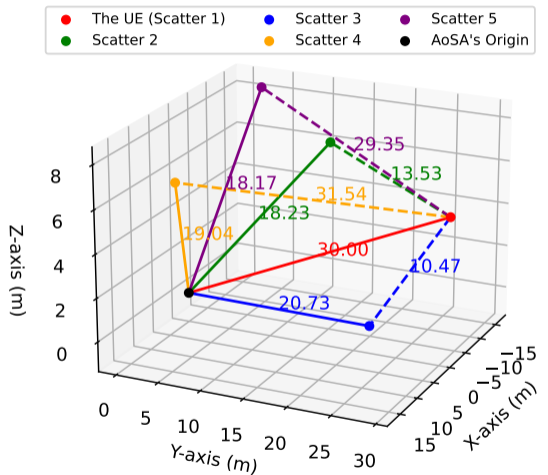
Near- and Far-field Radiation Regions



The Fraunhofer (Rayleigh) distance is commonly adopted to distinguish **near-field** and **far-field** regions, which is given by $D_F = 2D_A^2/\lambda_c$ and is increased with the aperture of the antenna array and the operating frequency, where D_A denotes the AoSA's array aperture, i.e., the diagonal length of the AoSA. If the receiver is located inside the Fraunhofer distance from the radiating unit, the **near-field** radiation characteristics should be considered and the wavefront has to be modelled as **spherical**.

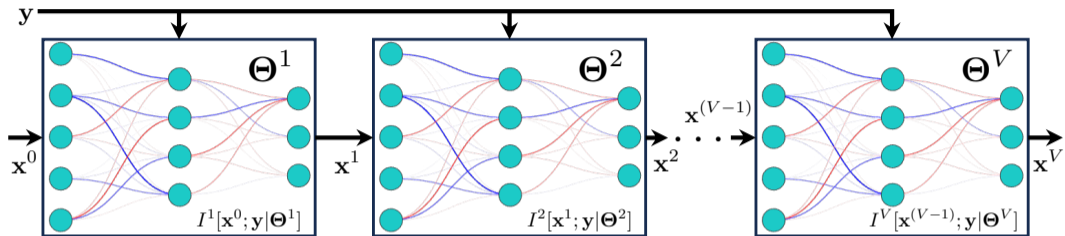
Cui, Mingyao, and Linglong Dai. "Channel estimation for extremely large-scale MIMO: Far-field or near-field?." IEEE TCom 70.4 (2022): 2663-2677.

Hybrid Near- and Far-Field THz Transmission



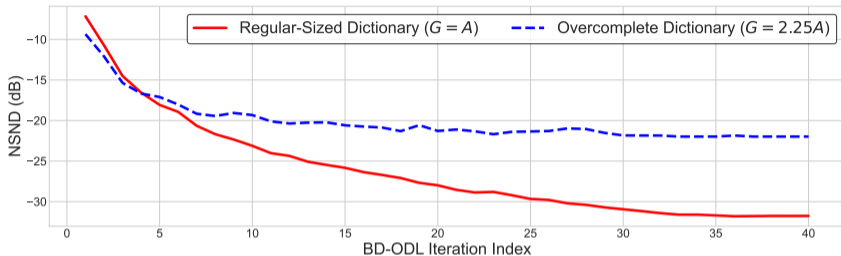
- In the multi-path propagation from the UE to the AoSA, there might be some scatters in the far-field, while some in the near-field.
- Therefore, the hybrid-field THz radiation is considered, where the overall THz channel consists of **portions** of near- and far-field paths.

How Deep Unfolding Works?

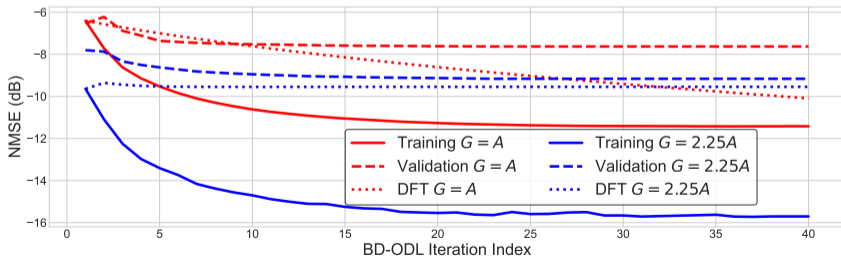


The training process aims to **minimize** the loss function, i.e., $\min_{\Theta} \Delta [x^V, x^*]$, in which $\Delta[\cdot, \cdot]$ is the loss function, $\Theta = \{\Theta^1, \Theta^2, \dots, \Theta^V\}$ denotes the set of each layer's trainable parameters, V measures the number of layers, x^* represents the ground-truth channel vector, $x^V = (I^V \triangleleft \dots \triangleleft I^2 \triangleleft I^1)[x^0; y | \Theta^V, \dots, \Theta^2, \Theta^1]$ captures the final output of the deep unfolding network after V -layer inference, and the symbol \triangleleft indicates the feed-forward process.

Training History of Batch-Delayed Online Dictionary Learning (BD-ODL)

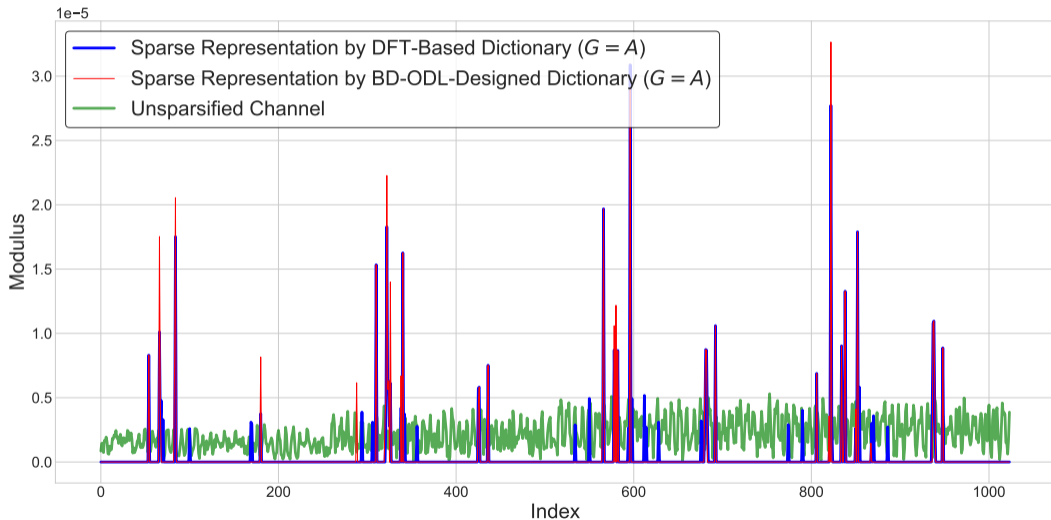


NSND:
Normalized
Square Norm
Difference

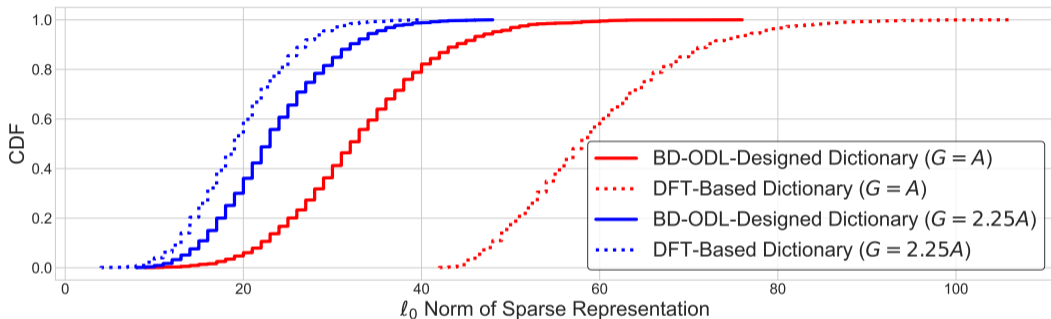


NMSE:
Normalized Mean
Squared Error

Element Modulus Curves versus Vector Index (Square Dictionary)

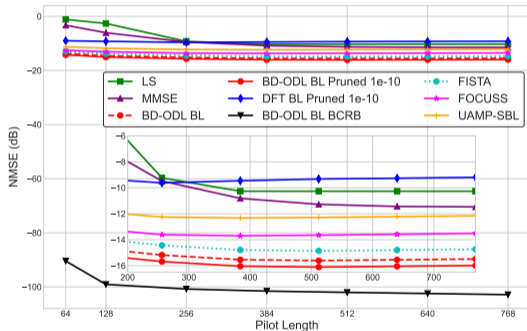


Cumulative Distribution Function (CDF) of the ℓ_0 Norms of the Sparse Representations



For instance, **90%** of the THz channel samples can be recovered by less than **44** or **72** atoms from the BD-ODL-designed or DFT-based dictionaries in the case of square dictionary, respectively. Note that the number of antenna element is **1024!**

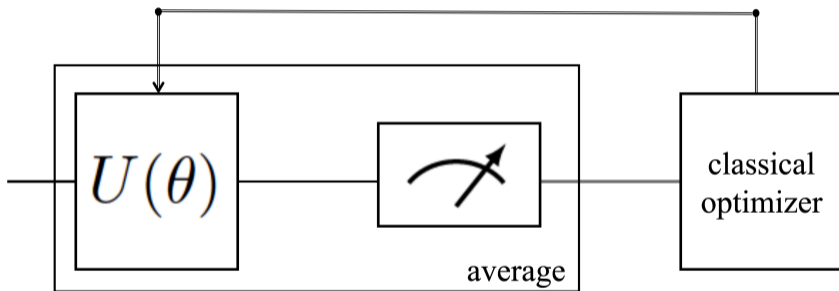
Normalized Mean Squared Error (NMSE) versus Pilot Length



- *LS*: The least square (LS) estimate.
- *MMSE*: The minimum mean square error (MMSE) estimate.
- *FOCUSS*: A typical sparse signal reconstruction algorithm that is popular in image recovery.
- *UAMP-SBL*: The approximate message passing (AMP) technique with unitary transformation is used to alternate the original E-step in SBL to reduce computational cost and enhance robustness.
- *FISTA*: The fast version of iterative shrinkage-thresholding algorithm (ISTA) which offers computational simplicity and global convergence rate.

What is Quantum Machine Learning (QML)?

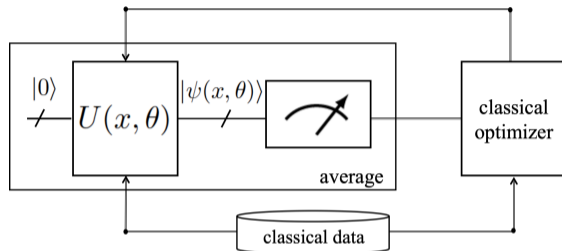
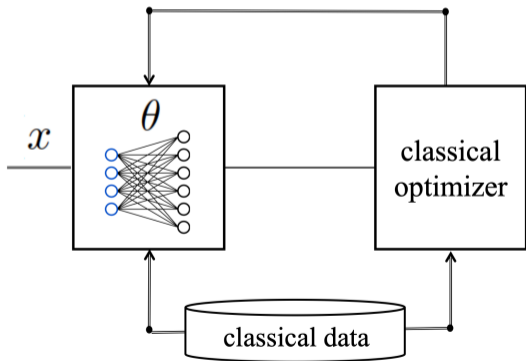
QML refers to a small-scale quantum circuit with a classical optimizer, in the noisy intermediate-scale quantum (NISQ) era.



A high-level description of the quantum machine learning design methodology. A parametric quantum circuit (PQC) implementing a unitary matrix $U(\theta)$ is optimized via its vector of parameters, θ , based on measurements of the output of the PQC.





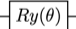

What is Quantum Machine Learning (QML)?

optimizing a standard machine learning model, such as a neural network, using a classical optimizer to minimize a cost function over parameters θ based on classical input data x .

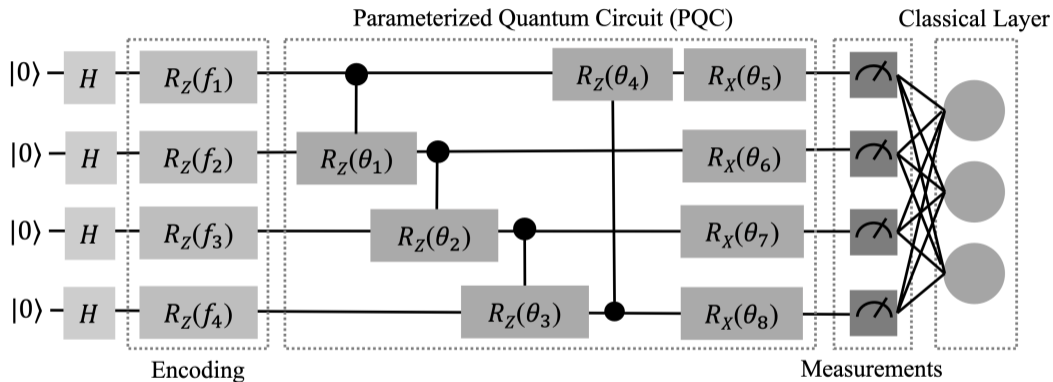


implements a unitary transformation $U(x, \theta)$ with the classical input x , and parameter θ
 the quantum circuit's input is a set of qubits in $|0\rangle$, leading to $|\psi(x, \theta)\rangle = U(x, \theta) |0\rangle$
 minimize the cost function over θ as per the estimate of an observable of the output quantum state $|\psi(x, \theta)\rangle$

Typical Quantum Gates

Gate Name	Unitary Matrix	Gate Symbol
Pauli's X	$X = \begin{bmatrix} 0 & 1 \\ 1 & 0 \end{bmatrix}$	
Pauli's Z	$Z = \begin{bmatrix} 1 & 0 \\ 0 & -1 \end{bmatrix}$	
Pauli's Y	$Y = iXZ = \begin{bmatrix} 0 & -i \\ i & 0 \end{bmatrix}$	
Hadamard	$H = \frac{1}{\sqrt{2}} \begin{bmatrix} 1 & 1 \\ 1 & -1 \end{bmatrix} = \frac{1}{\sqrt{2}}(X + Z)$	
Rotation (around y axis)	$R_y(\theta) = \begin{bmatrix} \cos(\theta/2) & -\sin(\theta/2) \\ \sin(\theta/2) & \cos(\theta/2) \end{bmatrix}$	
Controlled Not (CX)	$\begin{bmatrix} 1 & 0 & 0 & 0 \\ 0 & 1 & 0 & 0 \\ 0 & 0 & 0 & 1 \\ 0 & 0 & 1 & 0 \end{bmatrix}$	

An Example of Quantum Neural Network



Kundu, Satwik, and Swaroop Ghosh. "Security Concerns in Quantum Machine Learning as a Service." arXiv preprint arXiv:2408.09562 (2024).

Why Quantum Machine Learning?

- Quantum supremacy reported by IBM and Google, and the latest Nobel prize in Physics for ground-breaking experiments with quantum entangled particles, further reveal the promise and importance of quantum computing for leading the next industrial revolution.
- Quantum Machine Learning (QML) merges quantum computing with machine learning, leveraging entanglement and superposition for more efficient data processing.
- Quantum computing is beneficial for improving efficiency and enhancing generalization for ML systems, e.g., comparable or better learning performance with much lighter parameter updating of quantum DRL algorithm.

The Long-Term Interdisciplinary Vision!

$$\frac{1}{\sqrt{2}} |Wireless\rangle + \frac{1}{2} |ML\rangle + \frac{1}{2} |Quantum\rangle$$

The End

Thanks for your attentions

This is the end of today's talk